Optics and Photonics Journal, 2012, 2, 358-366
http://dx.doi.org/10.4236/opj.2012.24045 Published Online December 2012 (http://www.SciRP.org/journal/opj)

The Gain Distribution According to the Theoretical Structure and Decay Dynamics of Sodium-Like Cu

Wessameldin S. Abdelaziz[1], Mai E. Ahmed[2], Ali S. Khalil[3], Mohammed Alshaik Ahmed[4], Tharwat M. El-Sherbini[5]
[1]National Institute of Laser Enhanced Sciences, Cairo University, Giza, Egypt
[2]Environmental Affairs Agency, Cairo, Egypt
[3]Tebin Institute for Metrological Studies, Helwan, Egypt
[4]Al-Azhar University, Gaza, Palastine
[5]Laboratory of Lasers and New Materials, Cairo University, Giza, Egypt
Email: wessamlaser@yahoo.com

Received August 31, 2012; revised September 30, 2012; accepted October 10, 2012

ABSTRACT

Level structure, oscillator strengths, transition probabilities and radiative life times are evaluated for $1s^2\ 2s^2\ 2p^6 3l$, $4l$, $5l$ ($l = 0, 1, 2, 3, 4$) states in sodium-like Cu^{18+}. The calculations are carried out using COWAN code. The calculations were made are compared with other results in literature where a good agreement is found, we also report on some unpublished energy values and oscillator strengths. Our results are used in the calculation of reduced population of 21 fine structure levels over a wide rang of electron density values (10^{18} to 10^{20}) and at various electron plasma temperature. For those transitions with positive population inversion factor, the gain coefficients are evaluated and plotted against the electron density.

Keywords: Level Structure; Oscillator Strengths; Sodium-Like Cu

1. Introduction

Successful results on soft X-ray amplification have been achieved with the electron collisional excitation scheme including neon-like and nickel-like isoelectronic sequences [1-3]. With the neon-like scheme, the required pumping laser intensity increases rapidly as the wavelength be comes shorter towards the water window spectral region (4.4 - 2.3 nm) [4].

An important objective in the development of X-ray lasers is to deliver a coherent, saturated output at wavelengths toward the water window [1].

Such saturated X-ray lasers are required for holography [2] and microscopy [3], of biological specimens and for deflectometry [4], interferometry [5], and radiography [6] of dense plasma relevant to inertial confinement fusion and laboratory astrophysics [5]. Sodium-like ions have prominent emission lines in the UV and XUV spectrum of the sun. Highly charged sodium-like ions were observed in several types of laboratory sources such as high-voltage vacuum spark tokomak and laser-produced plasmas [1].

Spectra of these ions have a simple structure (one electron outside a closed shell); the energy levels are practically free from effects of configuration mixing and therefore they are well suited for a theoretical interpretation of line intensities and for diagnostic purposes. In recent years, there have been extensive spectroscopic studies, both experimental and theoretical, of sodium isoelectronic sequence. [7] have used multi-configuration Hartree Fock (MCHF) method and Non-Orthogonal Spline configuration interaction (CI) method to evaluate energy levels and oscillator strengths for Na-like ions up to Fe XVI. [8] have used theoretical single—configuretion Dirac-Fock method to evaluate oscillator strengths for E1 transitions in the sodium isoelectronic sequence (Na I-Ca X). Large-scale calculations were undertaken within the so-called Opacity Project (OP) [8] and, as a result of broad international collaboration, a complete set of oscillator strengths was produced for all optically allowed transitions between states with $1 \leq Z \leq 14$ as well as $Z = 16$, 18, 20, and 26 in all stages of ionization.

However, relativistic effects were also neglected in OP calculations and LS coupling was assumed. Therefore, the OP data are available for multiples only and not for individual fine-structure components. [9] assigned experimental wavelengths to 1086 lines which have oscillator strengths calculated in OP and added 1163 lines which have critically evaluated oscillator strengths. [10] and from the US National Bureau of Standards (NBS) publications [11-13]. Experimental lifetime measure-

ments for the 4p and 5p levels and calculation of transition probabilities in Na I have been measured using time-resolved laser induced fluorescence [14].

The purpose of this work is to present the energies of 21 fine structure levels, the Oscillator strengths, the transition probabilities between them in sodium-like Cu^{18+}.

The atomic data thus obtained are used to calculate reduced population of sodium-like Cu^{18+} excited levels over a wide range of electron density and at various electrons Temperatures. The gain coefficients are also calculated.

2. Computation of Atomic Structures

2.1. Model of Central Force Field

In quantum mechanics, various physical processes can be summed by Schrödinger equation, *i.e.*

$$H\Psi_i = E_i\Psi_i. \tag{1}$$

In the non-relativistic case (the influence of relativistic effect will be discussed later), the Hamiltonian of an atomic system with N electrons is:

$$\begin{aligned} H &= H_{kin} + H_{e-nuc} + H_{e-e} \\ &= \sum_i \frac{(h/2\pi)^2}{2m_e}\nabla_i^2 - \sum_i \frac{Ze^2}{r_i} + \sum_{i>j}\frac{e^2}{r_{ij}}. \end{aligned} \tag{2}$$

Here H_{kin}, $H_{e\text{-}nuc}$ and $H_{e\text{-}e}$ refer, respectively, to the kinetic energy of electrons, the Coulomb potential and the energy of electrostatic interaction of electrons, r_i is the distance between the i-th electron and nucleus, and $r_{ij} = |r_i - r_j|$.

By substituting the Hamiltonian into Schrödinger equation and solving the equation in the case of multiple electrons and multiple energy levels, the wave function is obtained. Now, due to the appearance of the term of interaction of electrons, an exact solution cannot be obtained. On the other hand, the interaction term is comparable with the Coulomb potential term, so it can by no means be ignored. An approximate solution is to adopt the method of central force field. If it is assumed that every electron moves in the central force field of the nucleus and also in the mean force field produced by other electrons, then we have the following effective Hamiltonian:

$$H^{eff} = \sum_i^N H_i^{eff} = -\sum_{i-1}^N \left[\frac{1}{2}\frac{p_i^2}{m_e} + \frac{Ze^2}{r_i} - V_i^{eff}(r_i)\right] \tag{3}$$

2.2. Method of Calculation

The key problem in the application of central field is to find an adequate potential function V^{eff}. For this, in recent decades many effective method of calculation have been developed. Among them the more important ones are the potential model, Hartree-Fock theory, the semi-empirical methods. In the following we present a brief introduction of semi-empirical methods.

Semi-empirical methods try to calculate atomic structures via solving the simplified form of the Hartree-Fock equation. The most typical is the Hartree-Fock-Slater method.

Afterwards, Cowan *et al*. revised this method and developed the RCN/RCG program used in our work. The merit of the program is its extreme effectiveness, and the shortcoming is its inability to estimate the precision.

2.3. Configuration Interaction

In the above-stated model of central force field, every electron can be described with a simple wave function. The overall wave function of atoms may be expressed with the following Slater determinant:

$$\varnothing = -\frac{1}{\sqrt{N!}}\begin{bmatrix} \varnothing_1(\aleph_1) & \cdots & \varnothing_1(\aleph_N) \\ \vdots & \ddots & \vdots \\ \varnothing_N(\aleph_1) & \cdots & \varnothing_N(\aleph_N) \end{bmatrix} \tag{4}$$

In reality, such a description is not very precise. The best wave function should be a linear combination of wave functions with single configurations, and these wave functions possess the same total angular momentum and spin symmetry. This method is called the interaction of configurations. In the computation of atomic structures, consideration of the configuration interaction is the basis requirement for a program.

2.4. Relativistic Correction

In a non-relativistic system, the oscillator strengths and dipole transitions under LS-coupling can be calculated. In calculating forbidden transitions, *jj*-coupling must be used, and for this relativistic effects have to be taken into account. Generally speaking, the effects may be treated in two ways. One is inclusion of Breit-Pauli operator in the non-relativistic equation, and other is direct solution of the Dirac equation. For the former, a mass velocity term, the Darwin term caused by the electric moments of electrons and the spin-orbit term are added to the Hamiltonian of the model of central force field [15]. For relativistic correction, the program RCN/RCG restore to the Breit-Pauli correction.

2.5. Weighted Oscillator Strengths and Lifetimes

The oscillator strength $f(\gamma\gamma')$ is a physical quantity related to line intensity I and transition probability $W(\gamma\gamma')$, as given by Sobelman [16]:

$$w(\gamma\gamma') = \frac{2w^2e^2}{mc^3}\left|f(\gamma\gamma')\right| \tag{5}$$

with, $I\alpha gW\left(\gamma\gamma^{\backslash}\right)\alpha g\left|f\left(\gamma\gamma^{\backslash}\right)\right|=gf$.

Here m = electron mass, e = electron charge, I = is initial quantum state, $W=\left(E(\gamma)-E\left(\gamma^{\backslash}\right)\right)/\hbar$, $E(\gamma)$ initial state energy, g = $(2J + 1)$ is the number of degenerate quantum state with angular momentum J (in the formula for initial state). Quantities with primes refer to the final state.

In the above equation, the weighted oscillator strength, gf, is given by Cowan [17]:

$$gf=\frac{8\pi^2 mca_0^2\sigma}{3h}S \tag{6}$$

where g is the statistical weight of lower level, f is the absorption oscillator strength, $\sigma=\left(E(\gamma)-E\left(\gamma^{\backslash}\right)\right)/hc$, h *is* Planck's constant, c = light velocity, and a_0 *is* Bohr radius, and the electric dipole line strength is defined by:

$$s=\left|\left\langle\lambda J\left\|P^1\right\|\gamma J^{\backslash}\right\rangle\right|^2 \tag{7}$$

This quantity is a measure of the total strength of the spectral line, including all possible transition between m, m' for different J_z Eigen states. The tensor operator P^1 (first order) in the reduced matrix element is the classical dipole moment for the atom in units of ea_0.

To obtain gf, we need to calculate S first, (or its square root):

$$s_{\gamma\gamma'}^{1/2}=\left|\left\langle\lambda J\left\|P^1\right\|\gamma J^{\backslash}\right\rangle\right| \tag{8}$$

In a multi-configuration calculation we have to expand the wave function $\left|\gamma J\right\rangle$ In terms of single configuration wave-functions, $\left|\beta J\right\rangle$ for both upper and lower levels:

$$\left|\gamma J\right\rangle=\sum\nolimits_{\beta}\gamma_{\beta J}^{\gamma}\left|\beta J\right\rangle \tag{9}$$

therefore, we can have the multi-configurationally expression for the square root of line strength:

$$S_{\gamma\gamma^{\backslash}}^{1/2}=\sum_{\beta}\sum_{\beta^{\backslash}}\gamma_{\beta J}^{\gamma}\left\langle\beta J\left\|P^1\right\|\beta^{\backslash}J^{\backslash}\right\rangle \tag{10}$$

The probability per unit time of an atom in specific state γJ to make a spontaneous transition to any state with lower energy is

$$P(\gamma J)=\sum A\left(\gamma J,\gamma^{\backslash}J^{\backslash}\right) \tag{11}$$

where $A\left(\gamma J,\gamma^{\backslash}J^{\backslash}\right)$ is the Einstein spontaneous emission transition probability rate, for a transition from the state. γJ to the state $\gamma^{\backslash}J^{\backslash}$

The sum is over all state $\gamma^{\backslash}J^{\backslash}$ with

$$E\left(\gamma^{\backslash}J^{\backslash}\right)<E(\gamma J).$$

The Einstein probability rate is related to gf with the following relation by [17]:

$$gA=\frac{8\pi^2e^2\sigma^2}{mc}gf \tag{12}$$

Since the natural lifetime $\tau(\gamma J)$ is the inverse of transition probability, then:

$$T(\gamma J)=\left(\sum A\left(\gamma J,\gamma^{\backslash}J^{\backslash}\right)\right)^{-1} \tag{13}$$

which is applicable to an isolated atom.

Interaction with matter or radiation will reduce the lifetime of any state.

3. Computation of Gain Coefficient

The possibility of laser emission from plasma of ions of various members of Na-like Cu via electron collisional pumping, in the XUV and soft X-ray spectral regions is investigated at different plasma temperatures and plasma electron densities.

The reduced population densities are calculated by solving the coupled rate equations [18-21].

$$\begin{aligned}&N_j\left[\sum_{i<j}A_{ji}N_e\left(\sum_{i<j}C_{ji}^d+\sum_{i>j}C_{ji}^e\right)\right]\\&=N_e\left[\sum_{i<j}N_iC_{ij}^e+\sum_{i>j}N_iC_{ij}^d\right]+\sum_{i>j}N_iA_{ij}\end{aligned} \tag{14}$$

here N_j is the population of level j, A_{ji} is the spontaneous decay rate from level j to level i, C_{ji}^e is the electron collisional excitation rate coefficient, and C_{ji}^d is the electron collisional de-excitation rate coefficient, which is related to electron collisional excitation rate coefficient by [22,23].

$$C_{ji}^d=C_{ij}^e\left[\frac{g_i}{g_j}\right]\exp\left[\Delta E_{ji}/KT_e\right] \tag{15}$$

where g_i and g_j are the statistical weights of lower and upper levels, respectively

The population of the j^{th} level is obtained from the identity [19,20,24],

$$N_i=\frac{\left[N_j\right]}{N_i}\frac{\left[N_i\right]}{N_t}\frac{\left[N_t\right]}{N_e}N_e \tag{16}$$

where N_I is the total number density of all levels of the ion under consideration, and N_t is the total number density of all ionization stage.

Since the populations calculated from Equation (14) are normalized such that [19,20,25]

$$\sum_{J=1}^{55}\left(\frac{N_J}{N_I}\right)=1 \tag{17}$$

where n is the number of all the levels of the ion under consideration.

Electron collisional pumping has been applied. Collision in the lasant ion plasma will transfer the pumped quanta to other levels, and resulted in population inversions then produced between the upper and lower levels.

Once a population inversion has ensured a positive gain through $F > 0$ [1].

$$F = \frac{g_u}{N_u}\left[\frac{N_u}{g_u} - \frac{N_l}{g_l}\right] \tag{18}$$

where $\frac{N_u}{g_u}$ and $\frac{N_l}{g_l}$ are the reduced populations of the upper level and lower level respectively. Equation (18) has been used to calculate the gain coefficient for Doppler broadening of the various transitions in the Na-like Cu ion.

$$\propto = \frac{\lambda_{lu}^3}{8\pi}\left[\frac{M}{\pi K T_i}\right]^{1/2} A_{ul} N_u F \tag{19}$$

where M is the ion mass, $\lambda_{\ell u}$ is the transition wavelength in cm, T_i is the ion temperature in $^{\circ}K$ and u, l represent the upper and lower transition levels respectively.

The gain coefficient is expressed in terms of the upper state density (N_u). This quantity depends on how the upper state is populated, as well as on the density of the initial source state. The source state is often the ground state for a particular ion.

4. Results and Discussions

4.1. Energy Levels

Adopting the program COWAN [17], we have computed the parameters of atomic structures of Cu XIX (**Table 1**). The energy levels considered in the calculation have 21 fine structures ranging from ground state $1s^2\ 2s^2\ 2p^6\ 3s$ to the excited states$1s^2\ 2s^2\ 2p^6\ 3d$, $1s^2\ 2s^2\ 2p^6\ 4s$, $1s^2\ 2s^2\ 2p^6\ 4d$, $1s^2\ 2s^2\ 2p^6\ 5s$, $1s^2\ 2s^2\ 2p^6\ 5s$, $1s^2\ 2s^2\ 2p^6\ 5d$, $1s^2\ 2s^2\ 2p^6$ 5 g even parity levels and $1s^2\ 2s^2\ 2p^6\ 3p$, $1s^2\ 2s^2\ 2p^6\ 4p$, $1s^2\ 2s^2\ 2p^6\ 4f$, $1s^2\ 2s^2\ 2p^6\ 5p$, $1s^2\ 2s^2\ 2p^6\ 5f$ odd parity levels.

Table 2 presents energy levels and fine-structure splitting for Cu^{18+} also presented the energy levels calculations of (Younis *et al*., 2006) the present calculations differ by less than 0.16% for most of the levels, they have used Configuration-Interaction Code (CIV3).and the differ from (Nist, 2009) by less than 0.14% for most of the levels, except in some cases like the levels 2, 3, 4, 5, 9 and 10 in which the percentage difference between our value and the last two calculations is (0.66%, 0.66%), (–1%, 0.28%), (0.35%, 0.27%), (0.3%, 0.35%), (–0.5%, 0.12) and (–0.49%, 0.13) respectively, This mean that our results are in a good agreement with the theoretical and experimental value.

Table 1. Parameters (in 1000 cm^{-1}) used in the HFR calculations for configurations of Cu^{18+}.

Parameter	Value
E_{av} 3s	0
E_{av} 3d	817.8918
ζ 3d	2.5716
E_{av} 4s	2538.6141
E_{av} 4d	2852.2149
ζ 4d	1.1058
E_{av} 5s	3631.0025
E_{av} 5d	3784.5436
ζ 5D	0.5686
E_{av} 5g	3826.6066
ζ 5g	0.0683
E_{av} 3p	355.1267
ζ 3p	23.4863
E_{av} 4p	2680.7844
ζ 4p	9.3163
E_{av} 4f	2926.6767
ζ 4f	0.2885
E_{av} 5P	3701.4463
ζ 5p	4.6147
E_{av} 5f	3822.256
ζ 5f	0.1487

4.2. Oscillator Strength and Transition Probability

In the present work we report results of oscillator strength and transition probabilities using the Cowan code taking relativistic corrections into account.

Table 3 presents the wavelength, transition probability and the values of oscillator strength with a comparison against another published paper (Younis *et al*., 2006 [26]) and NIST. There was good agreement with (NIST, 2009 [27) and only small differences about (0.8%) there was some similarities with the paper and high differences in some values about (85%).

4.3. Radiative Lifetime

Table 4 contains the present results of radiative lifetime for the upper and lower laser levels for the sodium-like Cu. The present calculations predict that the lifetime of the upper laser level must be longer than the lifetime of lower one to ensure the fast depletion of the population

Table 2. Calculated HFR energy levels and fine structure spliting (in 1000 cm^{-1}) for Cu^{18+}.

index	Level	Trem	$E_{cal.}$	$E_{[28]}$	$E_{[29]}$
1	$1s^2\ 2s^2\ 2p^6\ 3s$	$^2s_{1/2}$	0	0	0
2	$1s^2\ 2s^2\ 2p^6\ 3p$	$^2p_{1/2}$	331.64	329.436	329.436
3	$1s^2\ 2s^2\ 2p^6\ 3p$	$^2p_{3/2}$	366.87	370.758	365.826
4	$1s^2\ 2s^2\ 2p^6\ 3d$	$^2d_{3/2}$	814.034	811.14	811.791
5	$1s^2\ 2s^2\ 2p^6\ 3d$	$^2d_{5\backslash2}$	820.463	817.992	817.56
6	$1s^2\ 2s^2\ 2p^6\ 4s$	$^2s_{1/2}$	2538.614	2535.44	2535.44
7	$1s^2\ 2s^2\ 2p^6\ 4p$	$^2p_{1/2}$	2671.468	2667.49	2667.49
8	$1s^2\ 2s^2\ 2p^6\ 4p$	$^2p_{3/2}$	2685.443	2688.902	2681.6
9	$1s^2\ 2s^2\ 2p^6\ 4d$	$^2d_{3/2}$	2850.556	2865.349	2847
10	$1s^2\ 2s^2\ 2p^6\ 4d$	$^2d_{5\backslash2}$	2853.321	2867.269	2849.5
11	$1s^2\ 2s^2\ 2p^6\ 4f$	$^2f_{5/2}$	2926.1	2924.385	2924.4
12	$1s^2\ 2s^2\ 2p^6\ 4f$	$^2f_{7/2}$	2927.109	2925.41	2925.4
13	$1s^2\ 2s^2\ 2p^6\ 5s$	$^2s_{1/2}$	3631.003	3615.981	_ _ _ _ _
14	$1s^2\ 2s^2\ 2p^6\ 5p$	$^2p_{1\backslash2}$	3696.832	3693.4	3693.4
15	$1s^2\ 2s^2\ 2p^6\ 5p$	$^2p_{3\backslash2}$	3703.754	3695.943	3699.3
16	$1s^2\ 2s^2\ 2p^6\ 5d$	$^2d_{3\backslash2}$	3783.691	3779.55	3779.3
17	$1s^2\ 2s^2\ 2p^6\ 5d$	$^2d_{5\backslash2}$	3785.112	3780.434	3780.6
18	$1s^2\ 2s^2\ 2p^6\ 5f$	$^2f_{5\backslash2}$	3821.959	3818.201	3818.1
19	$1s^2\ 2s^2\ 2p^6\ 5f$	$^2f_{7\backslash2}$	3822.479	3818.624	3818.7
20	$1s^2\ 2s^2\ 2p^6\ 5g$	$^2g_{7\backslash2}$	3826.436	-	3823.1
21	$1s^2\ 2s^2\ 2p^6\ 5g$	$^2g_{9\backslash2}$	3826.743	-	3823.4

of lower level which helps the laser to sustain continuous or quasi-continuous wave operation.

4.4. Gain Distributions

4.4.1. Level Populations

The reduced population densities are calculated for 2 levels by solving the coupled rate equations (14) using the coupled equations CRMO code [28] for solving simultaneous coupled rate equations.

Our calculations for the reduced population as a function of electron densities are plotted in **Figures 1** and **2** at three different plasma temperatures (1/2, 3/4 of the ionization potential) for Na-like Cu.

We took into account in the calculation spontaneous radiated decay rate and electron collisional processes between all levels under study.

The behavior of level populations of the various ions can be explained as follows: in general, at low electron densities the reduced population density is proportional to the electron density, where excitation to an excited state is followed immediately by radiation decay, and collisional mixing of excited levels can be ignored.

At high densities ($N_e > 10^{20}$), radiative decay to all levels will be negligible compared to collisional depopulations and all level population become independent of electron density and approximately equal (see **Figures 1** and **2**). The population inversion is largest where electron collisional deexcitation rate for the upper level is comparable to radiative decay for this level [21].

Form our study, it was found that the gain coefficient was very low at (1/4 ionization potential) for all elements, so the results of gain coefficient and reduced population have not been mentioned.

4.4.2. Inversion Factor

As we mentioned before, laser emission will occur only if there is population inversion or in other words for

Table 3. Wavelength, oscillator strenghth and radiative rate for allowed transitions in Cu^{18+}.

	j	λ (Å)	*Aji* $(sec)^{-1}$	fijcal.	$Fij_{[28]}$
1	2	301.531	8.15E+09	0.1114	0.1083
1	3	272.576	2.21E+10	0.24602	0.2461
1	7	37.433	3.82E+11	0.08016	0.2106
1	8	37.238	7.75E+11	0.16105	0.4209
1	14	27.05	2.21E+11	0.02415	0.0168
1	15	27	4.43E+11	0.04841	0.0336
2	4	207.299	1.99E+10	0.25584	0.2737
2	6	45.311	2.01E+11	0.06194	0.0889
2	9	39.7	7.38E+11	0.34911	0.2178
2	13	30.309	8.95E+10	0.012302	0.0261
2	16	28.968	4.18E+11	0.10494	0.1572
3	4	223.631	3.18E+09	0.02371	0.0251
3	5	220.462	1.98E+10	0.21624	0.2305
3	6	46.046	3.84E+11	0.06094	0.0987
3	9	40.263	1.42E+11	0.03443	0.02407
3	10	40.218	8.52E+11	0.30969	0.2166
3	13	30.636	1.73E+11	0.01216	0.0283
3	16	29.267	8.10E+10	0.01039	0.0171
3	17	29.255	4.87E+11	0.09352	0.1542
4	7	53.838	6.63E+10	0.02877	0.08625
4	8	53.436	1.36E+10	0.005806	0.01736
4	11	47.347	2.80E+12	0.93742	0.7719
4	14	34.689	2.65E+10	0.00477	0.0000131
4	15	34.605	5.33E+09	0.00095	0.0000026
4	18	33.246	1.02E+12	0.16941	0.3043
5	8	53.62	8.05E+10	0.03466	0.1052
5	11	47.492	1.32E+11	0.04455	0.03689
5	12	47.469	2.63E+12	0.89093	0.7379
5	15	34.683	3.18E+10	0.00572	0.000004
5	18	33.317	4.83E+10	0.00805	0.01458
5	19	33.311	9.68E+11	0.161008	0.2918
6	7	752.706	1.89E+09	0.16068	0.146
6	8	681.067	5.10E+09	0.35478	0.3387
6	14	86.34	7.65E+10	0.08551	0.03472
6	15	85.827	1.56E+11	0.17177	0.06953
7	9	558.384	4.38E+09	0.40829	0.4317
7	13	104.217	6.45E+10	0.104705	0.001194
7	16	89.91	1.27E+11	0.30688	0.1081
8	9	605.643	6.85E+08	0.03757	0.03846
8	10	595.67	4.32E+09	0.3443	0.3502
8	13	105.757	1.23E+11	0.10302	0.002109
8	16	91.054	2.44E+10	0.03026	0.009396
8	17	90.936	1.47E+11	0.27286	0.08475
9	11	1323.74	3.78E+08	0.09952	0.09749
9	14	118.165	3.15E+10	0.06575	0.05316
9	15	117.206	6.45E+09	0.01327	0.01065
9	18	102.944	4.68E+11	0.74291	0.04293
10	11	1374.02	1.61E+07	0.00455	0.00449
10	12	1355.22	3.37E+08	0.09243	0.09151
10	15	117.587	3.83E+10	0.07922	0.06517
10	18	103.238	2.20E+10	0.03522	0.0021
10	19	103.182	4.42E+11	0.70607	0.04205
11	16	116.606	1.22E+10	0.01651	0.17251
11	17	116.413	5.82E+08	0.00118	0.01235
11	20	111.07	5.43E+11	1.33613	_____
12	17	116.55	1.16E+10	0.01773	0.1844
12	20	111.194	2.00E+10	0.03706	_____
12	21	111.156	5.61E+11	1.29991	_____
13	14	1519.09	6.00E+08	0.20795	0.1972
13	15	1374.55	1.62E+09	0.45916	0.4071
14	16	1151.29	1.37E+09	0.54446	0.4472
15	16	1250.98	2.14E+08	0.05011	0.0433
15	17	1229.13	1.35E+09	0.45913	0.3951
16	18	2613.16	1.74E+08	0.1778	0.1376
17	18	2713.97	7.38E+06	0.00816	0.0064
17	19	2676.17	1.54E+08	0.16551	0.1297
18	20	22335.1	1.10E+05	0.01093	_____
19	20	25272.9	2.80E+03	0.00026	_____
19	21	23451.3	9.83E+04	0.01013	_____

For simplicity, the $1s^2\ 2s^2\ 2p^6$ core is omitted in the identification.

Table 4. Radiative lifetime for Cu^{18+} laser levels.

Index	Level	life time (ns)
6	**4s ($^2s_{1/2}$)**	**1.70E−03**
7	**4p ($^2p_{1/2}$)**	**2.22E−03**

Table 5. Parameters of the most intense laser transitions in Cu^{18+} ion plasma.

Transition	Ion / Atomic data	Cu XIX
4p ($^2p_{1/2}$)→4s ($^2s_{1/2}$)	Wavelength λ (Å)	752.7
	Maximum gain α (cm^{-1})	0.079
	Electron density N_e (cm^{-3})	5.00E+19
	Electron temperature T_e (eV)	502.94

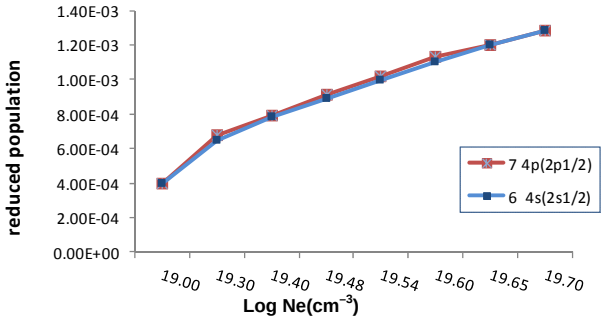

Figure 1. Reduced population of Cu^{18+} levels after electron collisional pumping as a function of the electron density at temperature 335.29.

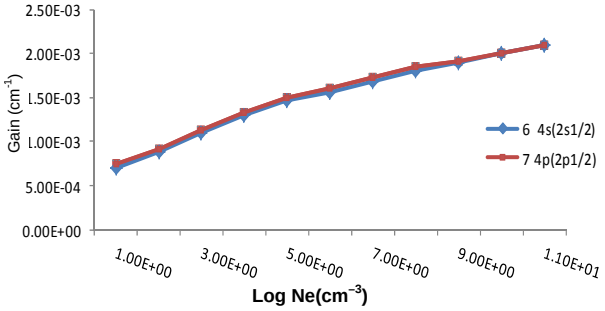

Figure 2. Reduced population of Cu^{18+} levels after electron collisional pumping as a function of the electron density at temperature 502.94.

positive inversion factor $F > 0$. In order to work in the XUV and X-ray spectral regions, we have chosen transitions between any two levels producing photons with wavelength between 30 and 1000 Å.The electron density at which the population reaches collisional equilibrium approximately equal to A/D, where A is radiative decay rate and D is the collisional deexcitation rate [20]. The population inversion is largest where the electron collisional deexcitation rate for the upper level is comparable to the radiative decay rate for this level.

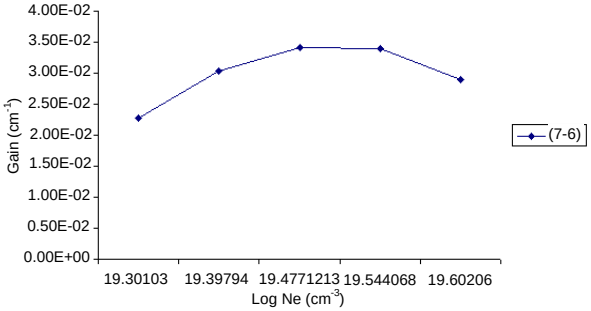

Figure 3. Gain coefficient of possible laser transitions against electron density at temperature 335.29 eV in Cu^{18+}.

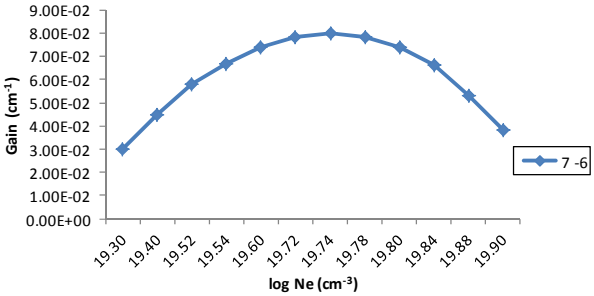

Figure 4. Gain coefficient of possible laser transitions against electron density at temperature 502.94 eV in Cu^{18+}.

For increasing atomic number Z, the population inversion occurs at higher electron densities, this is due to the increase in the radiative decay rate with Z and the decrease in collisional deexcitation rate coefficient with Z [29].

4.4.3. Gain Coefficient

As a result of population inversion there will be positive gain in laser medium. Equation (19) has been used to calculate gain coefficient for the Doppler broadening of various transitions in the Na-like Cu.

Our results for the maximum gain coefficient in cm^{-1} for those transitions having a positive inversion factor $F > 0$ in the case of Cu^{18+} ion at different temperatures are calculated and plotted against electron density in (**Figures 3** and **4**). The figures show that the population inversions occur for several transitions in the Cu^{18+} ion, however the largest gain occurs for the Cu^{18+} ion at $4p(^2p_{1/2})$-$4s(^2s_{1/2})$ transition.

For Na-like Cu, the population inversion is due to strong monopole excitation from the 3s ground state to the 3s 4d configuration and also the radiative decay of the 3s 4d level to the ground level is forbidden, while the 3s 4p level decays very rapidly to the ground level.

This short wavelength laser transitions was produced using plasmas created by optical lasers as the lasing medium. It is obvious that the gain increases with the temperature as the maximum gain increases with atomic number. Moreover, the peak of the gain curves shifts to

higher electron densities with the increase of atomic number.

5. Conclusion

The analysis that have been presented in this work shows that electron collisional pumping (ECP) is suitable for attaining population inversion and offering the potential for laser emission in the spectral region between 50 and 1000 Å from the Na-like Cu. This class of lasers can be achieved under the suitable conditions of pumping power as well as electron density. The positive gains obtained previously for some transitions in the ions under studies (Cu^{18+} ion) together with the calculated parameters could be achieved experimentally, then successful low cost electron collisional pumping XUV and soft X-ray lasers can be developed for various applications. The results have suggested the following laser transitions in the Cu^{18+} plasma ion, as the most promising laser emission lines in the XUV and soft X-ray spectral regions, **Table 5** gives parameters of the most intense laser transitions in Cu^{18+} ion plasma.

REFERENCES

[1] R. C. Elton, "X-Ray Lasers," Academic Press, New York, 1990, pp. 132-149.

[2] J. E. Trebes, S. B. Brown, *et al*., "Demonstration of X-Ray Holography and X-Ray Laser," *Science*, Vol. 238, No. 4826, 1987, pp. 517-519. doi:10.1126/science.238.4826.517

[3] L. B. Da Silva, J. E. Trebes, *et al*., "X-Ray Laser Microscopy of Rat Sperm Nuclei," *Science*, Vol. 258, No. 5080, 1992, pp. 269-271. doi:10.1126/science.1411525

[4] D. Ress, L. B. Da Silva, *et al*., "Measurement of Laser-Plasma Electron Density with a Soft X-Ray Laser Deflectometer," *Science*, Vol. 265, No. 5171, 1994, pp. 514-517. doi:10.1126/science.265.5171.514

[5] R. Cauble, L. B. Da Silva, *et al*., "Simultaneous Measurement of Local Gain and Electron Density in X-Ray Lasers," *Science*, Vol. 273, No. 5278, 1996, pp. 1093-1096. doi:10.1126/science.273.5278.1093

[6] D. H. Kalantar, M. H. Key, L. B. Da Silva, *et al*., "Measurement of 0. 35 Microm Laser Imprint in a Thin Si Foil Using an X-Ray Laser Backlighter," *Physical Review Letters*, Vol. 76, No. 19, 1996, pp. 3574-3577. doi:10.1103/PhysRevLett.76.3574

[7] C. F. Fischer, "A General Multi-Configuration Hartree-Fock Program," *Computer Physics Communications*, Vol. 14, No. 1-2, 1978, pp. 145-153.

[8] W. Siegel, J. Migdalek and Y. K. Kim, "Dirac-Fock Oscillator Strengths for E1 Transitions in the Sodium Isoelectronic Sequence (Na I-Ca X)," *Atomic Data and Nuclear Data Tables*, Vol. 68, No. 2, 1998, pp. 303-322.

[9] D. A. Verner, P. D Barthel and D. Tyther, "Atomic Data for Absorption Lines from the Ground Level at Wavelengths Greater than 228 A," *Astronomy and Astrophysics Supplement Series*, Vol. 108, No. 2, 1994, pp. 287-340.

[10] J. R. Fuhr and W. L. Wiese, "Atomic Transition Probabilities", In: D. R. Lide, Ed., *CRC Handbook of Chemistry and Physics*, 72th Edition, CRC Press, Boca Raton, 1991.

[11] W. L. Wiese, M. W. Smith and B. M. Miles, "Atomic Transition Probabilities, (Na through Ca-A Critical Data Compilation)," National Standard Reference Data Series (US), NSRDS-NBS 22, Vol. II, 1969.

[12] G. A. Martin, J. R. Fuhr and W. L. Wiese, "Atomic Transition Probabilities-Scandium: Through Manganese," *Journal of Physical and Chemical Reference Data*, Vol. 17, Suppl. 3, 1988.

[13] J. R. Fuhr, G. A. Martin and W. L. Wiese, "Atomic Transition Probabilities-Iron: Through Manganese," *Journal of Physical and Chemical Reference Data*, Vol. 17, Suppl. 4, 1988.

[14] R. M. Lowe and E. Biemont, "Lifetime Measurements for the 4p 2Po and 5p 3Po Levels and Calculation of Transition Probabilities in Na I," *Journal of Physics B*: *Atomic, Molecular and Optical Physics*, Vol. 27, No. 11, 1994, pp. 2161-2167. doi:10.1088/0953-4075/27/11/012

[15] D. R. Hartree and E. E. Salpeter, "Quantum Mechanics of One- and Two-Electron Atoms," Springer-Verlage, Berlin and New York, 1657.

[16] I. Sobelman, "Atomic Spectra and Radiative Transition," Springer, Berlin, 1979.

[17] R. D. Cowan, "The Theory of Atomic Structure and Spectra," University of California Press, Berkeley, 1981.

[18] U. Feldman, A. K. Bhatia, S. Suckewer, U. Feldman, A. K. Bhatia and S. Suckewer, "Short Wavelength Laser Calculations for Electron Pumping in Neon-Like Krypton (Kr XXVII)," *Journal of Applied Physics*, Vol. 54, No. 5, 1983, pp. 2188-2197. doi:10.1063/1.332371

[19] U. Feldman, J. F. Seely and G. A. Doschek, "3s-3p Laser Gain and X-Ray Line Ratios for the Carbon Isoelectronic Sequence," *Journal of Applied Physics*, Vol. 59, No. 12, 1986, pp. 3953-3957. doi:10.1063/1.336695

[20] U. Feldman, G. A. Doschek, J. F. Seely and A. K. Bhatia, "Short Wavelength Laser Calculations for Electron Pumping in Be I and B I Isoelectronic Sequences ($18 \leq Z \leq 36$)," *Journal of Applied Physics*, Vol. 58, No. 8, 1985, pp. 2909-2915. doi:10.1063/1.335838

[21] U. Feldman, J. F. Seely and A. K. Bhatia, "Scaling of Collisionally Pumped 3s-3p Lasers in the Neon Isoelectronic Sequence," *Journal of Applied Physics*, Vol. 56, No. 9, 1984, pp. 2475-2478. doi:10.1063/1.334308

[22] G. Chapline and L. Wood, "X-Ray Lasers," *Physics Today*, 28, No. 6, 1975, p. 40. doi:10.1063/1.3069004

[23] A. V. Vinogradov and V. N. Shlyaptsev, "Calculations of Population Inversion Due to Transitions in Multiply Charged Neon-Like Ions in the 200 - 2000 Å Range," *Soviet Journal of Quantum Electronics*, Vol. 10, No. 6, 1980, p. 754. doi:10.1070/QE1980v010n06ABEH010287

[24] U. Feldman, J. F. Seely and G. A. Doschek, "Short Wave-

length Laser Calculations in the Be I, B I and C I Isoelectronic Sequences," *Journal de Physique Archives*, Vol. 47, No. C6, 1986, pp. 187-202.

[25] M. J. Seaton, "Atomic Data for Opacity Calculations. I. General Description," *Journal of Physics B*: *Atomic and Molecular Physics*, Vol. 20, No. 23, 1987, p. 6363.

[26] W. O Younis, S. H Allam and Th. M. El-Sherbini, "Fine-Structure Calculations of Energy Levels, Oscillator Strengths, and Transition Probabilities for Sodium-Like Ions (Co XVII-Kr XXVI)," *Atomic Data and Nuclear Tables*, Vol. 92, No. 2, 2005, pp. 187-205.

[27] National Institute of Standards and Technology, Physical Reference Data, Atomic Spectra Database, Version 5, Vol. 11, 2009, pp. 3954-3958. http://www.nist.gov/pml/data/asd.cfm

[28] S. H. Allam, "CRMO Computer Code, Private Communication," 2003.

[29] U. Feldman, J. F. Seely and A. K. Bhatia, "Density sENSITIVE X-Ray Line Ratios in the Be_i, B_i, and Ne_i Isoelectronic Sequences," *Journal of Applied Physics*, Vol. 58, No. 11, 1984, pp. 3954-3958. doi:10.1063/1.335569

